Adaptive Nonlinear Stabilization Control for a Quadrotor UAV: Theory, Simulation and Experimentation

Mostafa Mohammadi · Alireza Mohammad Shahri

Abstract In this paper an adaptive control scheme along with its simulation, and its implementation on a quadrotor are presented. Parametric and non-parametric uncertainties in the quadrotor model make it difficult to design a controller that works properly in various conditions during flight time. Decentralized adaptive controller, which is synthesized based on improved Lyapunov-based Model Reference Adaptive Control (MRAC) technique, is suggested to solve the problem. The proposed control scheme does not need knowing the value of any physical parameter for generating appropriate control signals, and retuning the controller is not required for different payloads. An accurate simulation that includes empirical dynamic model of battery, sensors, and actuators is performed to validate the stability of the closed loop system. The simulation study simplifies implementation of the controller on our real quadrotor. A practical algorithm is proposed to alleviate and accelerate the tuning of controller parameters. The controller is implemented on the quadrotor to stabilize its attitude and altitude. Simulation and experimental results demonstrate the efficiency and robustness of the proposed controller.

Keywords Adaptive control · Stabilization · Decentralized control · Quadrotor · UAV

1 Introduction

Rotary wings unmanned aerial vehicles (UAV) have been used in a wide range of applications such as search and rescue operations, surveillance, and photography in recent years [1]. Because of the high maneuverability and simplicity of the mechanical structure, the quadrotor configuration has received more attention than other micro UAVs.

Attitude and altitude control of UAV lies at the heart of more complex control systems, like position control and obstacle avoidance [2]. Designing an efficient stabilizing controller involves coping with unmodeled dynamics, interaction between subsystems, inaccurate measurements, variable physical parameters, external disturbances, and mechanical underactuation [1]. So an advanced control scheme is required to achieve a high performance controller. In trying to reach this goal

M. Mohammadi (✉) · A. M. Shahri
Mechatronic & Robotic Research Laboratory,
Electronic Research Center, Electrical Engineering
Department, Iran University of Science
and Technology, Narmak 1684613114, Tehran, Iran
e-mail: mostafa.mohammadi90@gmail.com

A. M. Shahri
e-mail: shahri@iust.ac.ir

many researchers have solved the control problem for the quadrotor in various ways.

Orsag at [2] used an innovative method to get to the bottom of the Quadrotor control problem, which is based on a discrete automaton. This automaton combines classical PID and more sophisticated LQ controllers to create a hybrid control system. Using a simple nested saturation algorithm, [3] stabilized a quadrotor which is based on Layapunov analysis.

Adaptive control methods are used in [1, 4–6]. In [1, 4, 5] Backstepping Approach was used for controlling quadrotor. Some parametric and non-parametric uncertainties are considered in these papers. [6] developed an L1 adaptive output feedback control design process. This controller has robustness to time delay and Actuators Failure.

Intelligent control methods are presented in [7–9]. Dierks in [7] used Neural Networks to perform Output Feedback Control of a Quadrotor. Nicol at [8] proposed a new adaptive neural network control to stabilize a quadrotor in the present of modeling error and considerable wind disturbance. In [9] a fuzzy controller based on on-line optimization of a zero order TakagiSugeno fuzzy inference system, which is tuned by a back propagation-like algorithm, is applied to a quadrotor. In this paper some uncertainties are considered.

Robust approaches are utilized in [10–18]. Raffo in [10] used an integral predictive and H_∞ nonlinear robust control strategy to solve the path following problem for a quadrotor. Aerodynamic disturbances and parametric uncertainties are considered in this paper. Sliding mode control is employed to stabilize the quadrotor in [11, 13, 15, 18]. Feedback linearization control is used for controlling the quadrotor in [12–14]. Efe in [16] presented a robust control schemes that can alleviate disturbances. Fractional PID controller is proposed as a remedy. Cano in [17] presented Asynchronous networked control of quadrotor via L2-gain-based transformations.

Vision-based control algorithms of the quadrotor are discussed in [19–24]. These papers had used camera as well as AHRS to measure attitude and position. In [24] catadioptric system is utilized to estimate vehicle attitude in an urban environment. In order to increase the estimation and control speed an Extended Kalman Filter (EKF) was used.

For most of these references, except vision based control papers, the verification of the proposed algorithms has been limited to simulations and the model of actuators is not considered in their simulations studies either. In designing the controller, parametric and non-parametric uncertainties are not taken into account in order to achieve stability in close form altogether in the model.

Furthermore, important practical issues like battery discharging during flight time and variable mass have not received attention in the literatures. It is worth mentioning that despite the fact that the quadrotor structure and its weight are constant but its payload can be changed in various applications. So an adjustable feedback control is essential to have a decent performance despite different initial conditions and various situations during flight.

In this paper the dynamic model of the quadrotor, which is obtained by Lagrange-Euler formalism, is presented. A decentralized adaptive controller is proposed to stabilize the attitude and the altitude of a quadrotor in the presence of parametric and non-parametric uncertainties. In this approach, which is originally derived from [25], controlling each channel including roll, pitch, yaw, and altitude is performed independently while the effects of other channels are considered as a disturbance. There is no need to transfer information between the channels. Tuning the controller is not depends on the physical parameters of the UAV. Thus various payloads do not compel us to retune the controller. The stability proof of the control law is based on the improved Lyapunov-based Model Reference Adaptive Control (MRAC) technique. Furthermore, this paper focuses on using accurate simulation for ease of implementation and test on real platform. It is important because quadrotor's high speed propellers are dangerous and any crash can be very harmful and can damage the vehicle. So, almost complete model of the quadrotor is simulated to evaluate the performance of the proposed controller. This model includes dynamics equations of motion, aerodynamic forces and moments, and dynamics of actuators, battery and

sensors. The dynamic models of the battery, sensors and the actuators are obtained based on the experimental data. This leads to more profitable simulation results, which can accelerate controller implementation procedure on the real quadrotor. A well-structured quadrotor is designed and constructed. This quadrotor is stabilized by the proposed controller. An algorithm is suggested to tune the controller's parameters, which is one of the main contributions of this study. A wide range of experiments has been performed to ensure the capability of controller in various conditions.

Compared to other adaptive controllers that have been used to control quadrotor, which often based on backstepping technique and artificial neural networks, the proposed controller has simple structure. Furthermore, unlike artificial neural network based controllers there is no need to train the proposed controller.

The rest of the paper is structured as follows. The model of the quadrotor is presented in Section 2. Section 3 presents the overall control scheme. In Section 4 the quadrotor is simulated and the simulation results are presented. Section 5 gives hardware description, the proposed algorithm for controller parameters tuning, and experimental results. The summary of this work is given in the last section.

2 Quadrotor Dynamic Model

Having mathematical dynamic model of vehicle is essential for designing a good controller. Nevertheless, UAV model always includes some uncertainties. As the model becomes simpler, the controller becomes more complicated and a model with more details leads to more confident controller. UAV modeling procedure includes determining the dynamic equations of the vehicle body and the structure of uncertain dynamics, specifying the relationship between control inputs and outputs of actuators, and finally dynamics of actuators and sensors must be considered.

For obtaining the dynamic equations of quadrotor, as a 6DOF rigid body, the inertial frame and the body fixed frame should be defined. Let $B = \{B_1, B_2, B_3\}$ be the body fixed frame and $E = \{E_x, E_y, E_z\}$ be the inertial frame. The vector

$\xi = [x, y, z]^T$ is the position of UAV in inertial frame and the vector $\eta = [\phi, \theta, \psi]^T$ is the orientation of body frame with respect to fixed frame and called Euler angles. These angles are bounded as follows:

$$\begin{cases} roll: -\frac{\pi}{2} < \phi < \frac{\pi}{2} \\ pitch: -\frac{\pi}{2} < \theta < \frac{\pi}{2} \\ yaw: -\pi < \psi < \pi \end{cases} \tag{1}$$

The Lagrange-Euler rotational dynamics in terms of η can be expressed, as follows [3, 10]:

$$H(\eta)\ddot{\eta} + C(\eta, \dot{\eta})\dot{\eta} = \tau_\eta \tag{2}$$

τ_η represents the roll, pitch and yaw moments. The first term of left hand side of Eq. 2 represents the inertial moments while the second term includes Coriolis and centrifugal forces [27]. The elements of $H(\eta)$ and $C(\eta, \dot{\eta})$ are calculated in [10]. In translational dynamics in contrast to rotational dynamics there is gravitational potential energy. The translational dynamic equations can be expressed as follows [10]:

$$m\ddot{\xi} + mg \begin{bmatrix} 0 \\ 0 \\ E_z \end{bmatrix} = f_\xi \tag{3}$$

where m is the total mass of body and g is the gravity constant. f_ξ is a 3×1 vector containing all translational forces.

Some of the uncertain dynamics are Aerodynamic moments and forces and Friction forces. These forces and moments depend on velocities mostly [26]. We can express all uncertain forces and moments in unit terms $F_{\text{uncertain}}(\dot{\xi})$ and $\tau_{\text{uncertain}}(\dot{\eta})$ respectively. Therefore, dynamic equations of UAV are as follows:

$$\begin{cases} m\ddot{\xi} + mg \begin{bmatrix} 0 \\ 0 \\ E_z \end{bmatrix} = f_\xi + F_{\text{uncertain}}(\dot{\xi}) \\ H(\eta)\ddot{\eta} + C(\eta, \dot{\eta})\dot{\eta} = \tau_\eta + \tau_{\text{uncertain}}(\dot{\eta}) \end{cases} \tag{4}$$

As a propeller rotates in the air, it produces a force (thrust) and a moment (drag). Thrust and drag are denoted by T and D respectively. The direction of drag is opposite of rotation's direction. Both of them are proportional by square of rotational speed in the hover condition. We denote the force produced by rotors by T_1, T_2, T_3 and T_4. Moments produced by rotors are denoted by D_1,

D_2, D_3 and D_4. Since propellers 1 and 3 rotate in the opposite direction of propellers 2 and 4, then the signs of D_1 and D_3 are the opposite signs of D_2 and D_4 (See Fig. 1). When all rotors have the same rotation speed and the lift force is equal to the weight of the vehicle, then quadrotor has a fixed altitude and stable attitude. In this condition, the orientation of body frame with respect to the inertial frame is fixed, and the quadrotor is in the hovering mode. In order to change the altitude of quadrotor we must change the lift force which is defined by:

$$U = \sum_{i=1}^{4} T_i \qquad (5)$$

If T_1 and T_3 are not equal, the roll angle changes. Longitudinal movements also are achieved by change in roll angle. Thus the roll control input is defined as follows:

$$\tau_\phi = l(-T_1 + T_3) \qquad (6)$$

where l is the distance between center of rotor and center of vehicle (see Fig. 1). If T_2 and T_4 are not equal, the pitch angle changes. Lateral movements also are achieved by change in pitch angle. Thus

the pitch control input is defined as follows:

$$\tau_\theta = l(-T_2 + T_4) \qquad (7)$$

Yaw movement is obtained by change in sum of D_1, D_2, D_3 and D_4. As it mentioned previously, the signs of D_1 and D_3 are the opposite signs of D_2 and D_4. The yaw control input is defined as follows:

$$\tau_\psi = D_1 + D_2 + D_3 + D_4 \qquad (8)$$

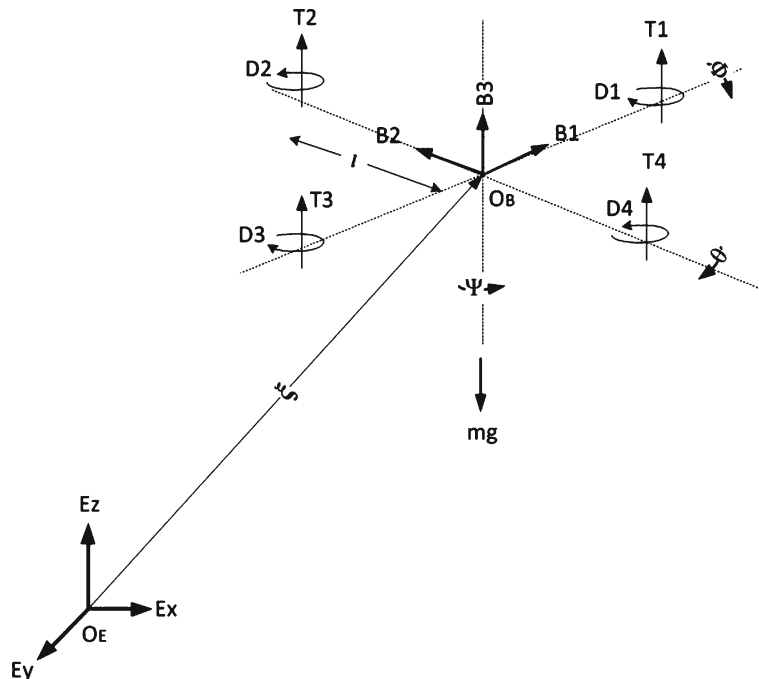So τ_η can be expressed as follows:

$$\tau_\eta = \begin{bmatrix} l(-T_1 + T_3) \\ l(-T_2 + T_4) \\ D_1 + D_2 + D_3 + D_4 \end{bmatrix} = \begin{bmatrix} \tau_\phi \\ \tau_\theta \\ \tau_\psi \end{bmatrix} \qquad (9)$$

By using the rotation matrix between the body fixed frame and the inertial frame, f_ξ can be expressed as follows [1]:

$$f_\xi = \begin{bmatrix} (S\psi S\phi + C\psi S\theta C\phi)\frac{U}{m} \\ (-C\psi S\phi + S\psi S\theta C\phi)\frac{U}{m} \\ (C\theta C\phi)\frac{U}{m} \end{bmatrix} \qquad (10)$$

Due to high power and low weight and fast response, brushless DC motors (BLDC) are

Fig. 1 Qaudrotor helicopter scheme

normally types of motors that are used in commercial UAV's. Due to very fast response of these motors the dynamic model of actuator in the control low synthesis is not considered. For simulation purpose, these types of actuators are modeled by experimental methods. The details of actuators modeling are described in the simulation section.

A quadrotor has six degrees of freedom. Since the number of actuators is less than the degrees of freedom we could not control all degrees of freedom simultaneously. These kinds of systems are called mechanical underactuated systems. In this paper, we want to control Altitude and attitude of quadrotor.

3 Controller Design

The altitude and attitude of the quadrotor is stabilized by decentralized adaptive controller. The desired altitude, roll, pitch and yaw are given to the quadrotor as inputs. The outputs of control loops are elements of F.

3.1 Decentralized Adaptive Control

By multiplying, the dynamic equations of UAV can be rewritten as:

$$m_i \ddot{q}_1 + d_i(q, \dot{q}, \ddot{q}) = F_i \quad i = 1...4 \quad (11)$$

In the proposed decentralized control scheme which is derived from [25], an independent controller is designed for each channel of Eq. 13. The control laws considered in this section are restricted to be decentralized, that's, each local controller operates solely on its own subsystem, with no exchange of information between the subsystems. The adaptive independent controller dedicated to the η_i and ξ_i are described by

$$F_i(t) = f_i(t) + (K_{0i}e_i(t) + K_{1i}(t)\dot{e}_i(t)) \ i = 1...4 \quad (12)$$

where $e_i = q_{ri} - q_i$ is state error. q_{ri} are desired values. The control law Eq. 14 is composed of two components, namely:

(i) The term $f(t)$ which is an auxiliary signal synthesized by the adaptation scheme to improve the tracking performance and partly compensate for the d_i.

(ii) The term $(K_{0i}(t)e_i(t) + K_{1i}(t)e_i(t))$ which is due to the adaptive feedback controller with adjustable gains $K_{0i}(t)$ and $K_{1i}(t)$, that acting on defined errors. The overall scheme of the control strategy is depicted in Fig. 2. The following Theorem gives the controller adaptation laws for tracking the desired trajectory that is produced by outer loops.

Theorem 1 *Consider the UAV dynamic equation Eq. 12 and Adaptive control low Eq. 14, the controller adaptation laws which ensure asymptotic trajectory tracking are based on the weighted error $r_i(t)$ as follows:*

$$r_i(t) = W_{pi}e_i(t) + W_{vi}\dot{e}_1(t) \quad (13)$$

Fig. 2 Quadrotor control scheme
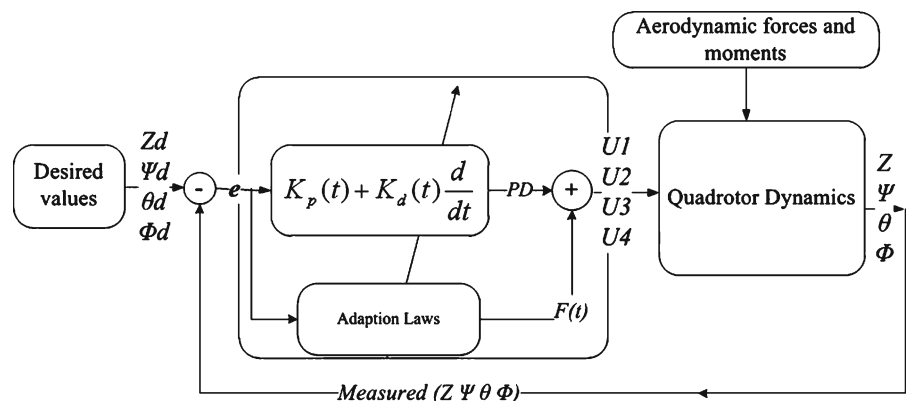
auxiliary signal:

$$f_i(t) = f_i(0) + \delta_i \int_0^t r_i(t)dt + \rho_i r_i(t) \qquad (14)$$

feedback gains:

$$K_{ij}(t) = K_{ij}(0) + \alpha_{ij} \int_0^t r_i(t)e_i^{(j)}(t)dt$$
$$+ \beta_{ij} r_i(t)e_i^{(j)}(t) \, j = 0, 1 \qquad (15)$$

where in $e_i^{(j)}(t)$ the superscript "(j)" denotes the jth derivative. δ_i, α_{ij} are any positive scalar integral adaptation gains, ρ_i, β_{ij} are zero or any positive proportional adaptation gains, and W_{pi}, W_{vi} are positive scalar weighting factors.

Proof The controller adaptation laws are derived using an improved Lyapunov based MRAC method. The controller synthesis and stability proof are given in [25].

$r_i(t)$ is a design parameter, which is used to tuning the controller. If the response is slow, W_{pi} must increase, and if more stable response is required, W_{vi} must increase.   ☐

4 Simulation

To assess the proposed non-linear adaptive controller, a simulation study with an almost complete model of the quadrotor is carried out. This model involves the dynamics equations of motion, aerodynamics equations, aerodynamics disturbances, and empirical dynamics of battery, motors, sensors. The most important result of performing this simulation scenario is that it leads to very fast tuning procedure of controller in practice. The following subsections are devoted to describing empirical model, simulation structure, and simulation results.

4.1 Simulation Structure

Desired altitude, roll, pitch, and yaw are given to controller by operator through a radio control receiver transmitter. Decentralized adaptive controller stabilizes the attitude and altitude of the vehicle. Then the control signals are converted to speed of motors and corresponding PWMs are applied to the motors. Tuning the controller Does not depend on the physical parameters of the UAV. In this simulation as previously mentioned, we consider empirical model for actuator. In the sensors modeling, white noise is considered according to sensors datasheets. Furthermore, discretization is performed both in time and values. The real mass properties of the quadrotor, which are obtained by SolidWorks®, are utilized for the simulation. Table 1 includes the mass and inertia parameters values of the quadrotor. Simulations are performed in Simulink®. The overall scheme of the control strategy is depicted in Fig. 3.

4.2 Empirical Actuator Modeling

The actuators of quadrotor are composed of a BLDC motor, its driver, and a propeller. The XM2830CA-14 Brushless DC motor, a product of DUALSKY®, with 12×4.7 propeller is used in this quadrotor. Each motor has Electronic Speed Controller (ESC), which receives command from the main controller in PWM form whose period is 4 ms and its duty cycle varies between 1 to 2 ms. The battery voltage is also reduced during the flight time with a little slope. Descending voltage of battery is an important issue that causes time-invariant controllers not to work properly and they need to be tuned in various initial conditions. Because the controller always generates PWM signal, while the constant PWM signal with variable voltage causes the motor to rotate in variable speed.

To avoid complexity in the model and to have a reliable model, a BLDC motor, its driver and a propeller are considered as a unique system. The voltage given to this module in PWM form.

Table 1 Values of the quadrotor physical parameters

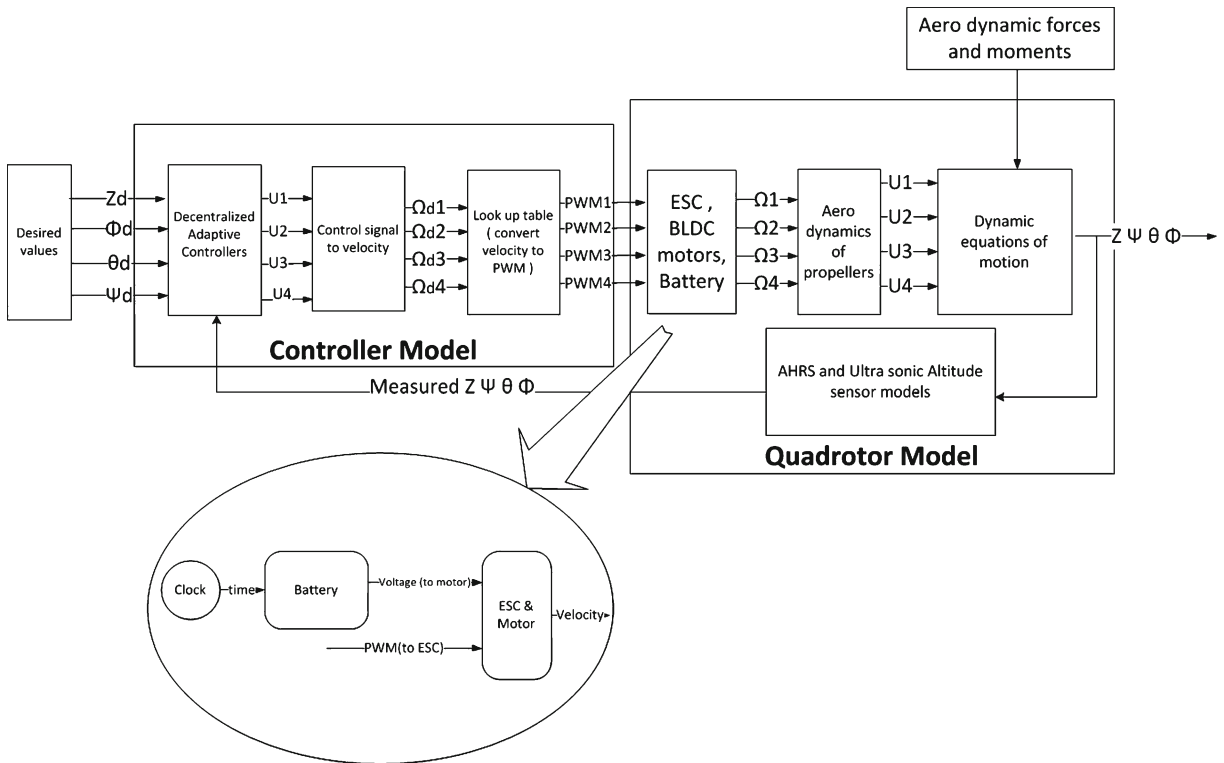| Parameter	Value	Unit
m	1.120	kg
I_{xx}	0.38	$m^2.kg$
I_{yy}	0.46	$m^2.kg$
I_{zz}	0.85	$m^2.kg$
l	0.24	m

Fig. 3 Quadrotor dynamic model along with decentralized adaptive controller simulation diagram

Output of this module is the of the propeller. The speeds of the motors can be changed between 0 rpm to 12,000 rpm by applying corresponding PWM to ESC. The propeller imposes a non-linear load on the motor. Having input and output data by using simple system identification methods, one can find relationship between voltage and speed and thrust factor. The relationship between voltage and speed is used for control purpose, i.e. proper motor speed is found by controller and the corresponding PWM is applied to motor.

To measure motor speed, CNY70 IR receiver/transmitter is used. Motor, which propeller attached to it, was installed on a fixed and tight structure. We measured motor speed by using a two color cover (black and white) on the outer side of motor. The sensor installed perpendicular to the motor, with keeping few distance (less than 10 mm). By measuring interval time of two consequential signals, which is received at two part of cover, the speed of the motor can be easily obtained.

The force is measured by FSH00980 load-cell, a product of FUTEK cooperation. This transducer is an S type load-cell. The load-cell was fixed on the floor. Motor was installed on top of the load-cell by screw, such that the motor can move in one direction. The displacement of motor due to force produced by propeller results in tension in load-cell. Output voltage of the load-cell is proportional to force. Note that good signal conditioning, and damping severe vibrations of the motor is essential to obtain useful results.

In order to find the thrust factor, the propeller's force is measured in various speeds. The relationship between force and rotation speed of the propeller is as follows.

$$F_T = K_T \Omega^2$$

where F_T is force, Ω is the rotation speed of the propeller, and K_T is the thrust factor. The gathered data and fitted curve are shown in Fig. 4.

Fig. 4 Measured forced,which is produced by the propeller, in various motor speeds
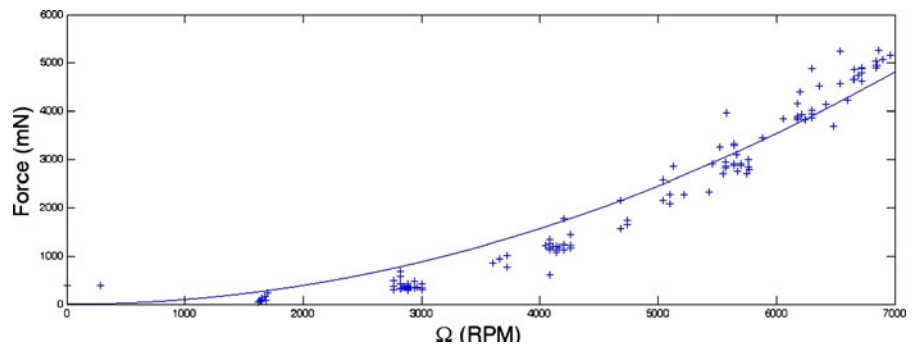
By using the least squares error method, the value of the thrust factor found. $K_T = 9.7 \times 10^{-5}$ In order to find the relationship between input of motor, i.e. PWM, and the speed of rotation, the rotation speed of the motor is measured in various PWMs. By using the least square technique a third order polynomial curve is fitted to the experimental data. The input and output data and fitted curve are depicted in Fig. 5.

$$f(x) = p_3 \times x^3 + p_2 \times x^2 + p_1 \times x + p_0$$

Its coefficients values are obtained as follows:

$$p_3 = 1.115 \times 10^{-5}, \ p_2 = -0.06572,$$

$$p_1 = 130.8, \ p_0 = -76230$$

For the battery modeling we also use the experimental data. The maximum voltage of the battery drops to minimum voltage during flight time t_{flight} gradually. A linear function shows the output of the voltage of battery according to flight time (for our quadrotor flight time is 15 min), the minimum voltage is 10 volt and the maximum voltage is 13 volt.

$$voltage(t)$$

$$= \left(maximumvoltage \right.$$

$$\left. - \frac{maximumvoltage - minimumvoltage}{t_{\text{flight}}} t \right)$$

$$/ maximumvoltage$$

4.3 Simulation Results

The control objective is to make the quadrotor hover at an altitude of 40 cm. its initial altitude is

Fig. 5 Measured rotational speed of the motor in various PWMs
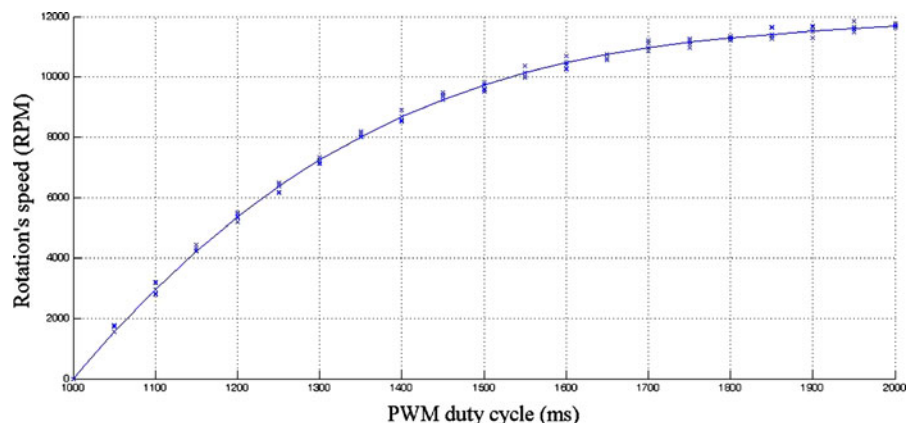
90 cm. The initial values of controller parameters were determined as follows:

$$f(0) = [0, 0, 0, 0]$$

$$k_{i0}(0) = [48, 48, 48, 85]$$

$$k_{i1}(0) = [32, 32, 32, 58]$$

The positive constants of the controller are determined as follows:

$$W_p = diag(6.25, 6.25, 6.25, 25),$$

$$W_v = diag(1, 1, 1, 5)$$

$$\alpha_{i1} = [0.72, 0.72, 1.2, 5],$$

$$\alpha_{i2} = [0.02, 0.02, 0.14, 3.2]$$

$$\beta_{i1} = [2, 2, 10, 32], \beta_{i2} = [0.5, 0.5, 1.2, 10]$$

$$\delta = [0.005, 0.005, 0.01, 0.04], \rho = [0, 0, 0, 0]$$

Figure 6 depicts the altitude and attitude responses of the simulated quadrotor with the pro-posed decentralized adaptive controller. It can be seen that each channel remains at a set-point very close despite interconnection between channels. Figure 7 shows the four control signals, which are generated by adaptive controllers. As it can be seen it the Fig. 7 the weight of the quadrotor is compensated by U1. It means that U1 causes motors produce a force, which its average is equals to the weight of the quadrotor. Three other control signals stabilize the attitude of the quadrotor. Since the quadrotor operate near hover condition these control signals are usually smaller than U1. These fine signals need to be accurate and very fast in order to stabilize the system. Thus, we use a 14 bit timer/counter to generate the PWMs for motors. It is important to note that PWM's duty cycle, which changes between 1 to 2 ms, generated by a 14 bit timer/counter. The values of control signal change between 0 to $2^{14}(16384)$, so the control signal equal to 0 means duty cycle of PWM is 1 ms, and if the control signal equals to 16384, its corresponding duty cycle is 2 ms.
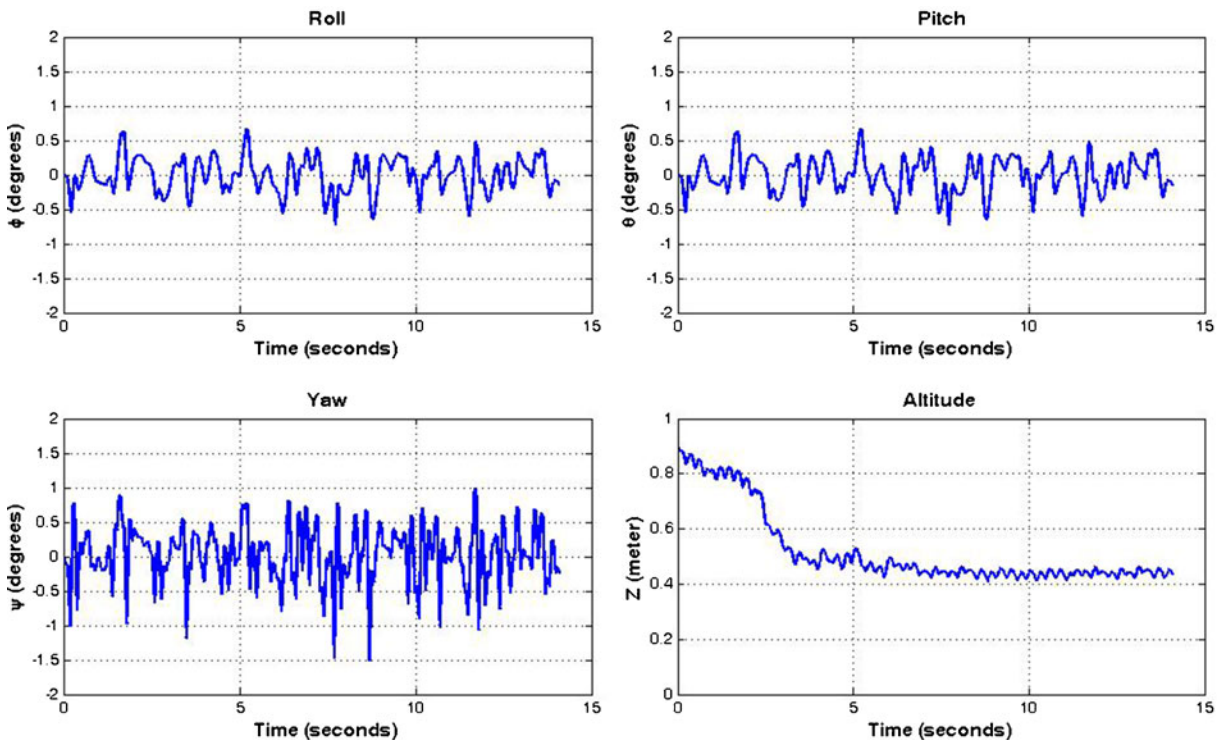

Fig. 6 Altitude and attitude responses of the simulated quadrotor with decentralized adaptive controllers
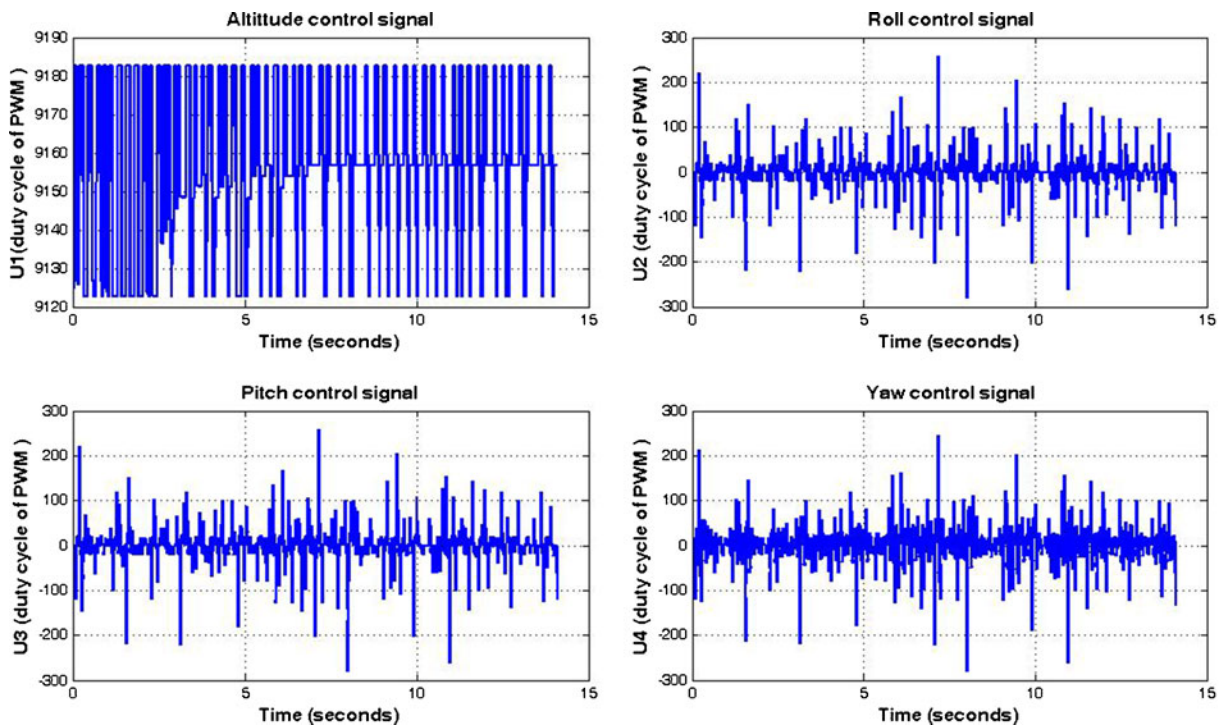
Fig. 7 Control signals generated by decentralized adaptive controllers to stabilize the simulated quadrotor

5 Experimentation

This section describes our quadrotor platform briefly at first. In the following subsection, an efficient algorithm has been proposed to simplify the implementation of feasible controllers. The experimental results are illustrated in the last part of this section.

5.1 Hardware Description

The structure of our platform is made of carbon fiber (65 cm × 65 cm × 25 cm). Its total weight is 1,210 gr with payload capacity about 250 gr permits 15 min flight duration (see Fig. 8). Its avionic architectures as shown in Fig. 9 is completely modular. The Arm microcontroller gathers

Fig. 8 The quadrotor platform

Fig. 9 Modular avionic architecture of the quadrotor
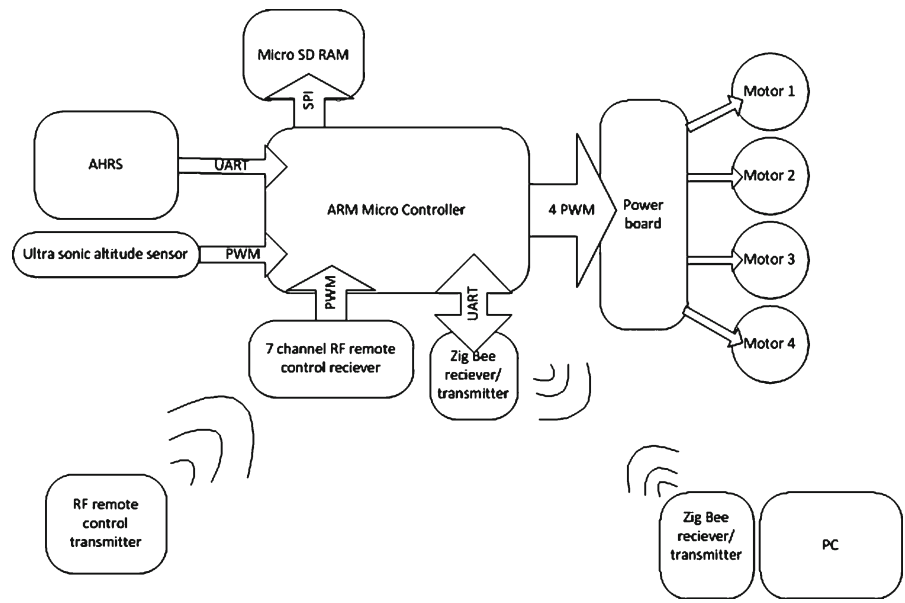
data of Attitude and Heading Reference System (AHRS) and ultra-sonic sensor. Four control signals are transmitted by a radio control transmitter to an ARM microcontroller. In order to simplify tuning of the controller and for flight security reasons, we have introduced some switches in remote control. The control signals are calculated according to the introduced control scheme, and then speed commands are given to the brushless DC motor drivers in PWM form. All sensors data, input commands, and state of controller are stored in the micro-SD RAM for analysis and fault detection after probable crashes. Also, all data are sent to the base station through a wireless network (IEEE 802.11). The base-station is implemented on a PC at core2Due 2.5 GHz with a 3 GB RAM. The system is monitored by a simple Matlab software. The components of avionic system, which are shown in Fig. 10, are as follows; STM32F103RB microcontroller is chosen as flight

Fig. 10 Avionic components: **a** main control board with ARM microcontroller, **b** AHRS, **c** ultrasonic, **d** zig-bee receiver/transmitter, **e** radio control, **f** brushless DC motor
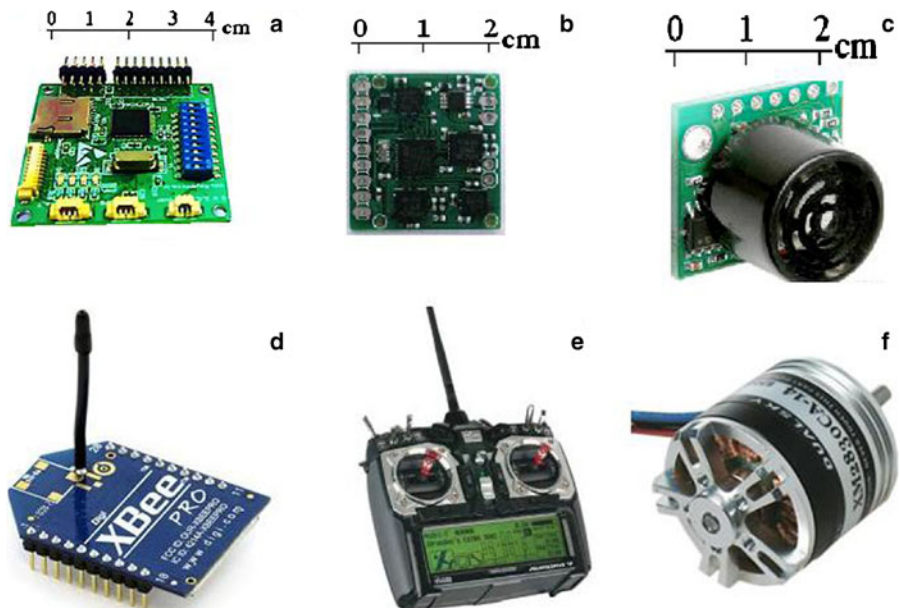
computer of our quadrotor. It incorporates high performance ARM Cortex-M3 32-bit RISC core operating at a 72 MHz maximum frequency (for our purpose 16 MHz is enough.), high speed embedded memories, an extensive range of enhanced I/Os and peripherals connected to two APB buses, two 12-bit ADCs, and 7 timers plus 9 communication interfaces (I2C, USART, SPI, CAN, USB). This choice enables us to extend the system in a simple way for advanced missions. The CHR-6dm AHRS is a cost-effective orientation sensor providing yaw, pitch, and roll angle outputs at up to 300 Hz. An Extended Kalman Filter (EKF) combines data from onboard accelerometers, rate gyros, and magnetic sensors to produce yaw, pitch, and roll angle estimates. The LV-MaxSonar®-EZ1™, which detects objects from 0-inches to 254-inches, is used as indoor altitude sensor. The interface output formats included are pulse width output, analog voltage output, and serial digital output. The XM2830CA-14 brushless DC motor a product of DUALSKY®is used in this quadrotor. It has low weight (55 gr) and high power (200 watt). Their power is provided by 2200 mAh 3S 11.1 V Li-Po battery. A 7-channel 2.4 GHz Radio Control transmitter is used to send commands to the quadrotor.

5.2 Controller Parameters Tuning

Tuning the simple controllers, which have constant coefficients, consist of changing the coefficients over and over to find the best response of the system in this configuration (mass properties and voltage of battery). However if the mass properties is changed, for example by adding a camera to your drone, or when the voltage of the battery decreases, the tuned coefficients do not work ideally and the system need to retune. The proposed controller simplifies the tuning process in two ways; first finding the initial coefficient (on the test bench) is easier. Because, the controller is self-tuning and find the best values for coefficients by itself. Second when the mass properties or voltage of battery changed there is no need to retune the controller. For controller tuning the following

algorithm, which is depicted in Fig. 11, is proposed as follows:

1. *Configure Software* this step consists of two main stages:

   (a) Initialization and configuration of Data Acquisition system, e.g. determining sampling rate, filtering, etc. The data acquisition system gathers data of AHRS, ultrasonic and radio control receiver.
   (b) Motors initializing and configuration, e.g. command rate, resolution of PWM, etc.

2. *Tune each rotational controller individually* in this step you need a test bench to limit the degrees of freedom of the quadrotor to one degree. The quadrotor must have the ability to rotate around one axis, e.g. roll. Then, the controller of the selected channel must be tuned. Tuning of the controller to each channel involves two stages, tuning with zero command, and test with non-zero command. It is essential to test the controller with non-zero command, because the behaviour of the system is completely different in large angles (bear in mind that the quadrotor is non-linear system). It is vital to test the controller with various commands to find the maximum command that the system can tolerate, especially for linear controllers, which are designed based on small angle approximation. This step can be divided into three stages:

   (a) Tune the roll controller channel
      i. Tune the roll channel controller with zero constant command
      ii. Test the roll channel controller with variable commands
   (b) Tune the pitch controller channel
      i. Tune the pitch channel controller with zero constant command
      ii. Test the pitch channel controller with variable commands
   (c) Tune the yaw controller channel
      i. Tune the yaw channel controller with zero constant command
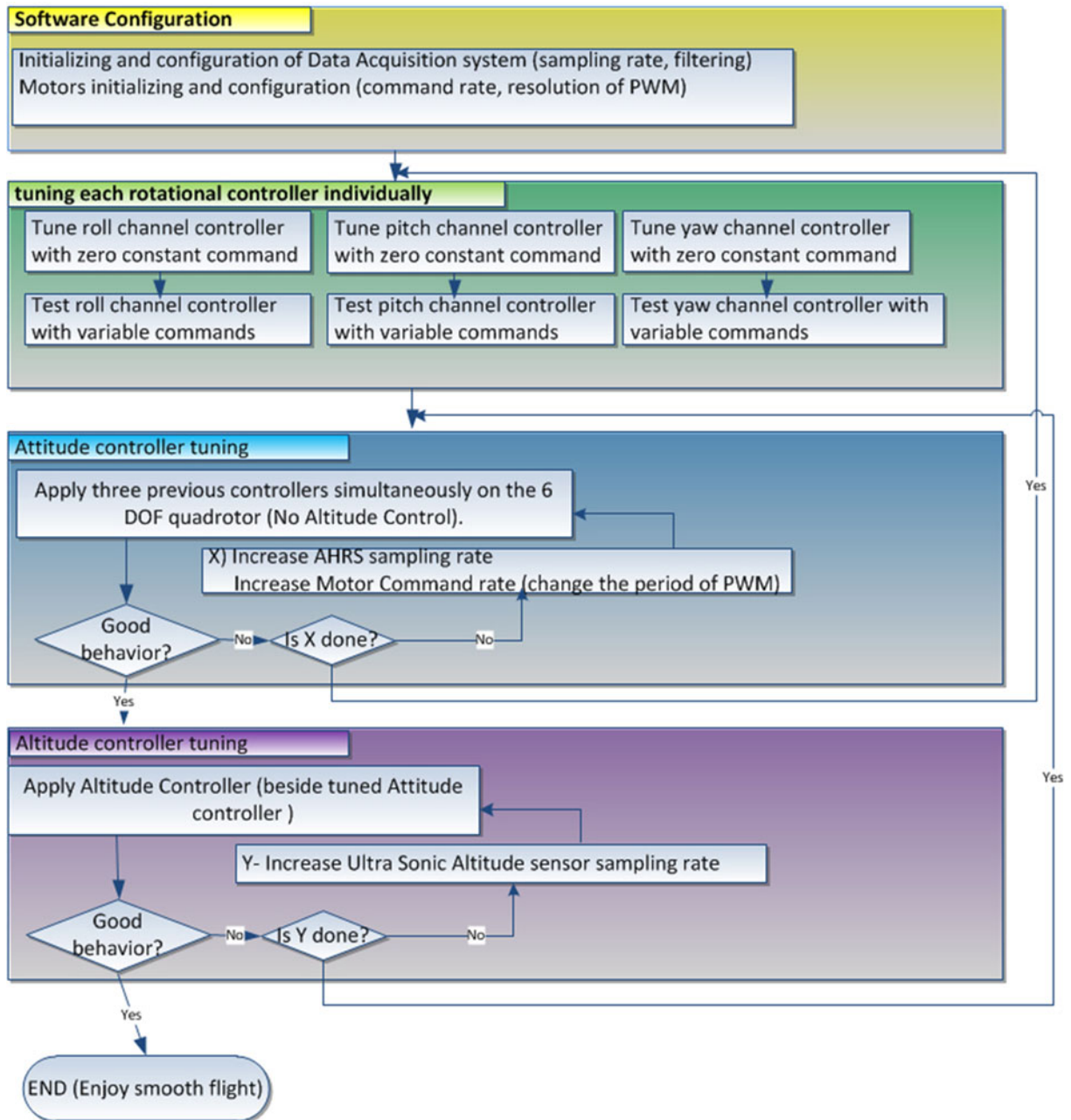   ii. Test the yaw channel controller with variable commands

Fig. 11 Proposed algorithm to tuning parameters of stabilizing controller for a quadrotor UAV

3. *Tune the attitude controller* after performing the previous step, implement all three controllers on 6 DOF quadrotor altogether. If the system demonstrates good behaviour, i.e. can be hovered easily, go to the next step.

Otherwise, if the controller does not show good behaviour and you previously did not increase the AHRS sampling rate and the motors command rates enough, raise them. If you change them several times and the controller

does not have good behaviour, go back to step 2 and modify the controller structure.

4. *Tune the altitude controller* when the attitude controller is tuned well, apply the altitude controller to quadrotor. If the system demonstrates good behaviour, i.e. can be hovered easily, and the operator does not sense a lot of vibration and sudden movement, and commands are performed smoothly, algorithm is done. Otherwise, if controller does not have good behaviour and you previously did not increase ultra-sonic altitude sensor sampling rate enough, raise it. If you change it several times and the system does not exhibit good behaviour, go back to step 3 and modify the attitude controller.

5.3 Experimental Results

The experimental results include 2 groups of tests; a group for classic PID controller [26],

and another for proposed adaptive controller. Each group of tests includes three tests; first test with nominal weight and full battery, second test with payload and full battery, and third test with low voltage battery (its own battery after 8 min flight). These tests show that simple controller does not work in various conditions properly and need to retune while the proposed adaptive controller find the proper coefficient, tune itself and its performance better than classic PID controller.

The initial values for the control parameters were determined based on the empirical actuator model and we set the values such that, the thrust force be equal to weight of quadrotor.

$$f(0) = [0, 0, 0, 0]$$

$$k_{i0}(0) = [25, 25, 25, 70]$$
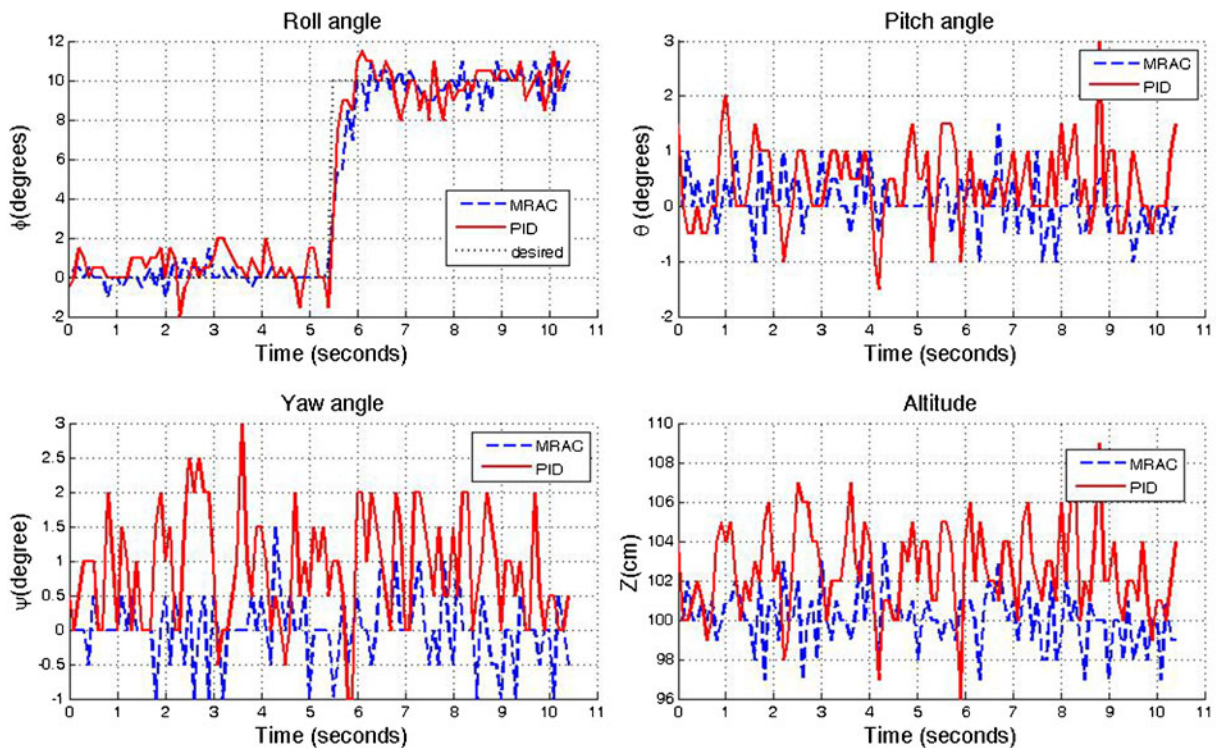
$$k_{i1}(0) = [17.5, 17.5, 35, 50]$$

Fig. 12 Quadrotor step response to adaptive and classic controllers (full battery, without payload)

The constant parameters of the controllers are determined as follows:

$$W_p = diag(10, 10, 14, 40), W_v = diag(1, 1, 2, 5)$$

$$\alpha_{i1} = [0.175, 0.175, 0.35, 1],$$

$$\alpha_{i2} = [0.0035, 0.0035, 0.35, 1]$$

$$\beta_{i1} = [0, 0, 0, 50], \beta_{i2} = [0, 0, 0, 10]$$

$$\delta = [0.001, 0.001, 0.0025, 0.01], \rho = [0, 0, 0, 0]$$

Figures 12, 13 and 14 show the response of the adaptive and classic controller to the 10° step input for the roll channel with constant value for other three channels ($pitch = 0\ deg$, $yaw = 0\ deg$, $altitude = 1$ m) with full battery and without payload, with full battery and with 200 gr payload, and with low battery and without payload respectively.

High rotational speeds of the propellers cause the severe vibration of the mechanical structure. Although the amplitude of these vibrations is small, but the high sensitive AHRS measured them and appropriate control signal are generated by the controllers. In order to reduce these inevitable vibrations, a mechanical damper is put under the AHRS. It is worth mentioning that different digital Low-Pass Filters (LPF) are examined to remove the high frequency noises but, time delay arising from use of the LPFs cause to instability of the system instead of improving its behaviour.

The controllers were tested in various conditions, the performance of the controllers in static and dynamic behaviour were compared by three factors; Performance index, which is defined as sum of squire errors, Overshoot, and Settling time. As it can be seen from the Figs. 12, 13, 14 and Table 2 for the proposed adaptive controller the
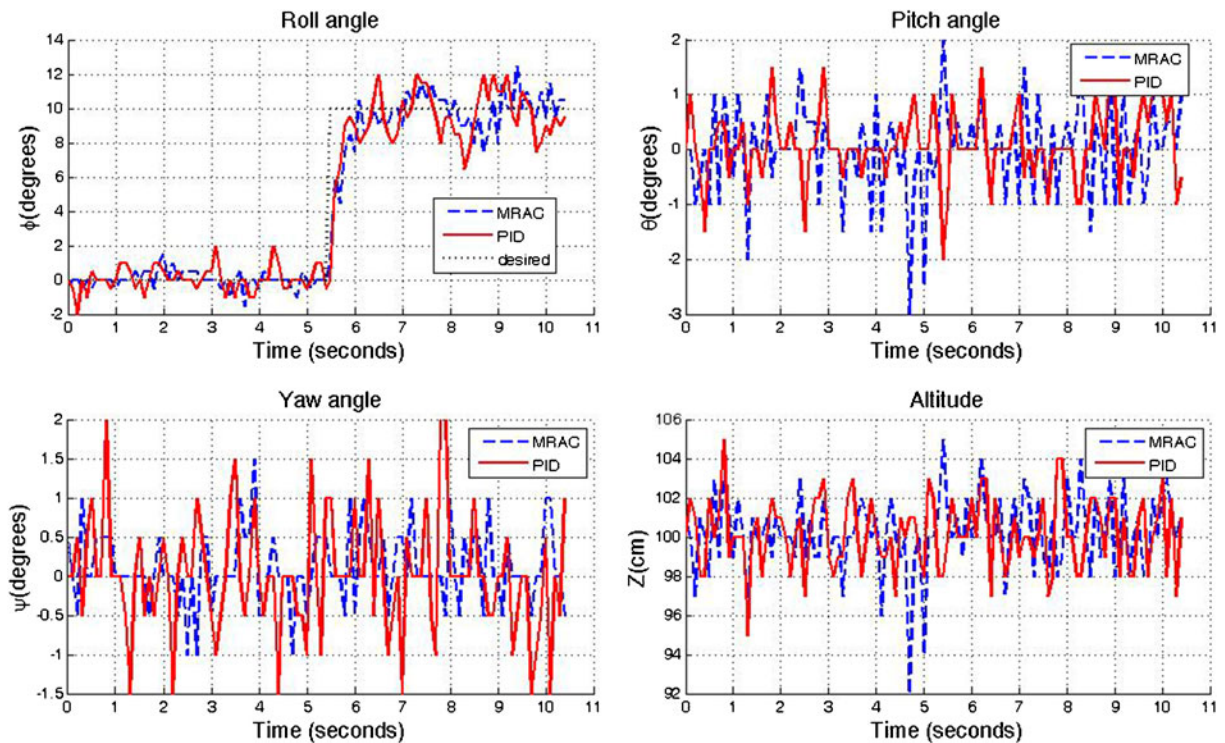

Fig. 13 Quadrotor step response to adaptive and classic controllers (full battery, with 200 gr payload)
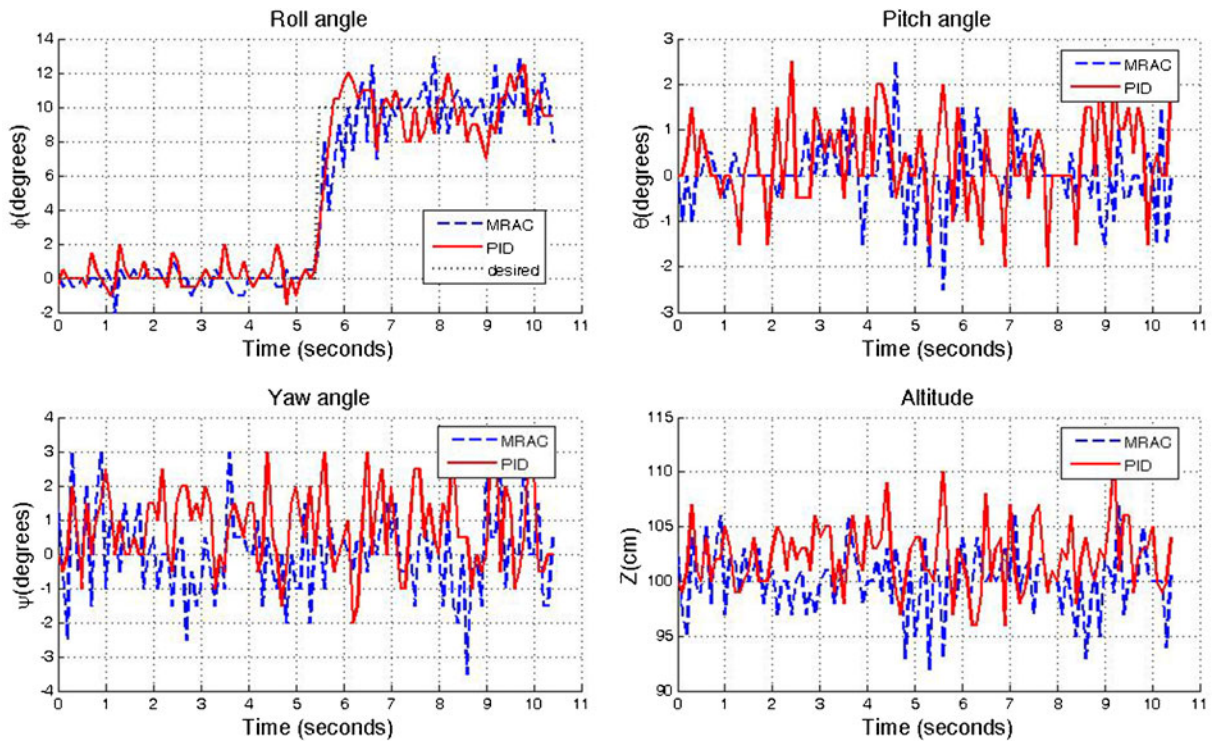
Fig. 14 Quadrotor step response to adaptive and classic controllers (low battery, without payload)

performance index, overshoot and settling time are better than classic PID controller.

Another interesting point is: the performance index for adaptive controller changed less than classic PID controller in various condition. the performance index for classic controller has 66 % variation from nominal condition to loaded condition and has 49 % variation from nominal condition to low battery condition, while the adaptive controller has 50 and 38 % variation in performance index in the mentioned conditions respectively

6 Conclusion

A decentralized adaptive controller has been proposed to stabilize the attitude and altitude of the quadrotor. In designing the controller, both parametric and non-parametric uncertainties of model

Table 2 Performance comparison between decentralized adaptive controller and classic PID controller

	Decentralized adaptive Controller	PID Controller
Full battery without payload	Performance index=134.75 Overshoot=10 % settling time=0.6	Performance index=153 Overshoot=15 % settling time=1
Full battery with 200 gr payload	Performance index=202.75 Overshoot=5 % settling time=0.6	Performance index=253.5 Overshoot=20 % settling time=1
Low battery without payload	Performance index=185.25 Overshoot=20 % settling time=0.9	Performance index=228 Overshoot=20 % settling time=1.2

are considered in close form. Improved Lyapunov based on model reference adaptive control analysis is employed to prove that the system is globally asymptotically stable.

A new vehicle is designed and built, and the control algorithm is implemented on it. Accurate simulation, which is based on empirical model, and proposed consecutive algorithm make it simple to implement and tune the controller. Simulation and experimental results confirm the high capability of proposed controller in stabilizing the quadrotor. Now the system can be effectively used in more complicated tasks.

References

1. Das, A., Lewis, F., Subbaro, K.: Backstepping approach for controlling a quadrotor using lagrange form dynamics. J. Intell. Robot. Syst. **56**(1–2), 127–151 (2009). doi:10.1007/s10846-009-9331-0

2. Orsag, M., Poropat, M. Bogdan, S.: Hybrid fly-by-wire quadrotor controller. Automatika **51**(1), 19–32 (2010)

3. Castillo, P., Dzul, A., Lozano, R.: Real-time stabilization and tracking of a four-rotor mini rotorcraft. IEEE Trans. Control Syst. Technol. **12**(4), 510–516 (2004). doi:10.1109/TCST.2004.825052

4. Madani, T., Benallegue, A.: Adaptive control via backstepping technique and neural networks of a quadrotor helicopter. In: Proceedings of the 17th World Congress the International Federation of Automatic Control, pp. 6513–6518. Seoul, Korea (2008)

5. Huang, M., Xian, B., Diao, C., Yang, K., Feng, Y.: Adaptive tracking control of underactuated quadrotor unmanned aerial vehicles via backstepping. In: Proceedings of American Control Conference, pp. 2076–2081. Marriott Waterfront, Baltimore, MD, USA (2010)

6. Michini, B., How, J.: L1 adaptive control for indoor autonomous vehicles: design process and flight testing. In: Proceeding of AIAA Guidance, Navigation, and Control Conference, pp. 5754–5768. Chicago, Illinois (2009)

7. Dierks, T., jagannathan, S.: Output feedback control of a quadrotor uav using neural networks. IEEE Trans. Neural Netw. **21**(1), 50–66 (2010)

8. Nicol, C., Macnab, C.J.B., Ramirez-Serrano, A.: Robust adaptive control of a quadrotor helicopter. J. Mechatronics **21**(6), 927–938 (2011)

9. Zemalache, K., Maaref, H.: Controlling a drone: Comparison between a based model method and a fuzzy inference system. Appl. Soft Comput. **9**, 553–562 (2009). doi:10.1016/j.asoc.2008.08.007

10. Raffo, G., Ortega, M., Rubio, F.: An integral predictive/nonlinear H_∞ control structure for a quadrotor helicopter. Automatica **46**, 29–39 (2010). doi:10.1016/j.automatica.2009.10.018

11. Mhammed, G., Hicham, M.: A high gain observer and sliding mode controller for an autonomous quadrotor helicopter. Int. J. Intell. Control Syst. **14**(3), 204–212 (2009)

12. Das, A., Lewis, F., Subbaro, K.: Dynamic inversion with zero-dynamics stabilisation for Quadrotor control. IET Control Theory Appl. **3**, 303–314 (2009). doi:10.1049/iet-cta:20080002

13. Lee, D., Kim, H., Sastry, S.: Feedback linearization vs. adaptive sliding mode control for a quadrotor helicopter. Int. J. Control Autom. **7**(3), 419–428 (2009). doi:10.1007/s12555-009-0311-8

14. Benallegue, A., Mokhtari, A., Fridman, L.: High-order sliding-mode observer for a quadrotor UAV. Int. J. Robust Nonlinear Control **18**(4–5), 427–440 (2008). doi:10.1002/rnc.1225

15. Zhang, R., Quan, Q., Cai, K.Y.: Attitude control of a quadrotor aircraft subject to a class of time-varying disturbances. IET Control Theory Appl. **5**(9), 1140–1146 (2011). doi:10.1049/iet-cta.2010.0273

16. Efe, M.Ö.: Neural network assisted computationally simple PID control of a quadrotor UAV. IEEE Trans. Ind. Informat. **7**(2), 354–361 (2011). doi:10.1109/TII.2011.2123906

17. Cano, J.M., Lo' pez-Mart'nez, M., Rubio, F.R.: Asynchronous networked control of linear systems via L2-gain-based transformations: analysis and synthesis. IET Control Theory Appl. **5**(4), 647–654 (2011). doi:10.1049/iet-cta.2010.0205

18. Fahimi, F, Saffarian, M.: The control point concept for nonlinear trajectory-tracking control of autonomous helicopters with fly-bar. Int. J. Control **84**(2), 242–252 (2011). doi:10.1080/00207179.2010.549842

19. Guenard, N., Hamel, T., Mahony, R.: A practical visual servo control for an unmanned aerial vehicle. IEEE Trans. Robot. **24**(2), 331–340 (2008). doi:10.1109/TRO.2008.916666

20. Mahony, R., Corke, P., Hamel, T.: Dynamic image-based visual servo control using centroid and optic flow features. J. Dyn. Syst. Meas. Control. **130**, 35–46 (2008). doi:10.1115/1.2807085

21. Bourquardez, O., Mahony, R., Guenard, N., Chaumette, F., Hamel, T., Eck, L.: Image-based visual servo control of the translation kinematics of a quadrotor aerial vehicle. IEEE Trans. Robot. **25**(3), 743–749 (2009). doi:10.1109/TRO.2008.2011419

22. Garca Carrillo, L.R., Rondon, E., Sanchez, A., Dzul, A., Lozano, R.: Stabilization and trajectory tracking of a quadrotor using vision. J. Intell. Robot. Syst. **61**(1–4), 103–118 (2011). doi:10.1007/s10846-010-9472-1

23. Eberli, D., Scaramuzza, D., Weiss, S., Siegwart, R.: Vision based position control for mavs using one single circular landmark. J. Intell. Robot. Syst. **61**(1–4), 495–512 (2011). doi:10.1007/s10846-010-9494-8

24. Tarhan, M., Altug, E.: EKF based attitude estimation and stabilizationof a quadrotor uav using vanishing points in catadioptric images. J. Intell. Robot. Syst. **62**(3–4), 587–607 (2011). doi:10.1007/s10846-010-9459-y

25. Seraji, H.: Decentralized adaptive control of manipulators: theory, simulation, and experimentation. IEEE Trans. Robot. Autom. **5**(2), 183–201 (1989)

26. Bouabdallah, S.: Design and control of quadrotor with application to autonomous flying. Unpublished Doctoral Dissertation, pp. 15–25. EPFL University, Lausanne (2007)

27. Asada, H., Slotine, J.: Robot Analysis and Control. Wiley, New York (1986)